# Hardware optimization on Android for inference of AI models

Iulius Gherasim

Carlos García Sánchez

Department of Computer Architecture and Automation Complutense University of Madrid Madrid, Spain 0009-0009-2479-0960 Department of Computer Architecture and Automation Complutense University of Madrid Madrid, Spain 0000-0002-3470-1097

Abstract—The pervasive integration of Artificial Intelligence models into contemporary mobile computing is notable across numerous use cases, from virtual assistants to advanced image processing. Optimizing the mobile user experience involves minimal latency and high responsiveness from deployed AI models with challenges from execution strategies that fully leverage real time constraints to the exploitation of heterogeneous hardware architecture. In this paper, we research and propose the optimal execution configurations for AI models on an Android system, focusing on two critical tasks: object detection (YOLO family) and image classification (ResNet). These configurations evaluate various model quantization schemes and the utilization of ondevice accelerators, specifically the GPU and NPU. Our core objective is to empirically determine the combination that achieves the best trade-off between minimal accuracy degradation and maximal inference speed-up.

Index Terms- Artificial Intelligence, Heterogeneous Computing, GPU, NPU, SoC, Performance, YOLO, ResNet, Android

# I. INTRODUCTION

In recent years, Neural Network models have revolutionized numerous domains by providing intelligent solutions for process automation and resource optimization. However, as Artificial Intelligence (AI) systems transition from research prototypes to large-scale commercial applications, computational cost and energy consumption have become major concerns. The inference phase, where models operate continuously, dominates this consumption. Specifically, Google estimates that AI-related tasks accounted for 10-15% of its total energy use between 2019 and 2021, with inference consuming 60% of that energy [1]. Similarly, Meta reports an energy capacity distribution of 10:20:70 for experimentation, training, and inference, respectively [2]. This consumption trend is steep: Google's energy usage grew 21% annually over the past decade, and Meta's grew even faster at 32% annually [3], [4].

The escalating demands of AI workloads have driven the evolution of computing personal systems away from homogeneous processors toward heterogeneous architectures. This approach integrates multiple processing units, such as CPUs, GPUs, TPUs, and specialized accelerators, within a single system to optimize performance and energy efficiency by assigning tasks to the unit best suited for them. Furthermore, these advances are critical to the emerging Edge-to-Cloud

paradigm [5]–[8]. In this model, data is processed locally at the "Edge" when possible, optimizing latency and bandwidth, while complex processing is offloaded to the "Cloud".

In the contemporary mobile computing landscape, AI performance is a core differentiator. The increasing complexity of AI models, pushed by the rapid popularization of AI [9], demands execution that meets strict real-time and accuracy requirements. Initial solutions involved offloading computation to the GPU, but recently approaches has been move to the use of specific domain-specific-architecture (DSA) as NPUs for this specific task. This DSA is engineered specifically to accelerate the tensor operations that dominate AI model layers, achieving better results in both compute speed and energy efficiency. Along with advancements on hardware, numerous frameworks emerged to allow developers to make use of artificial intelligence in their applications such as Pv-Torch, ONNX and TensorFlow. However, when mobile devices became powerful enough TensorFlow Lite, an extension of TensorFlow with select operations, enabled local execution on the device itself of certain lightweight models. As of 2024, TensorFlow Lite has been rebranded into LiteRT, short for Lite RunTime, and in the near future it will be renewed again to LiteRT Next as Google keeps adding functionality to the framework, with the main focus being native support for accelerator offloading of model operations.

In the context of benchmarking, MLPerf [10] was created to evaluate Machine Learning (ML) inference systems - from embedded devices to data centers - to decouple software frameworks and architecture neutral. Our work specifically adopts MLPerf principles to evaluate performance on mobile devices based on SoC of a commercial Android device. We selected two industry-standard models that are core components of the MLPerf benchmark suite and are essential for real-world vision systems: ResNet [11] for Image Classification and the YOLO family [12] for Object Detection. The choice of ResNet and YOLO provides a representative evaluation, contrasting a fundamental classification task with the real-time, complex demands of object detection, thereby generating robust data that reflects the needs of current, energy-efficient applications.

The manuscript is structured as follows: Section II describes topics related to Android's table environment used in this work;

Section III describes the methodology for this study; Section IV presents the results obtained, including performance comparisons; and Section V summarizes our contributions and proposes future research directions.

# II. ENVIRONMENT

# A. Hardware aspects

All the experimentation has been carried out in a stock Android tablet device, namely a Samsung Galaxy Tab S9. This device has been chosen as it comes with a System-of-Chip (SoC) which includes a NPU alongside the GPU and CPU, the devices that will be evaluated in this paper. The specific SoC is a Qualcomm Snapdragon SM8550-AC also referred to as Snapdragon 8 Gen 2 Mobile Platform. There are the three main computing units inside the SoC of interest for this paper, CPU, GPU and NPU, alongside other smaller dedicated units for networking or image processing.

The SoC CPU, named *Kryo*, is made up of eight cores arranged in a big.LITTLE configuration, with five *big* cores and three *little* cores. The name of each one and their maximum frequency is listed in table I. Of those cores, the three *little* ones are ARM Cortex-A510 cores, the first generation of high efficiency cores from the ARMv9 series of processors running at up to 2 GHz. The *big* cores on the other hand are not five of the same type of processor, instead being made up of three different kinds of ARM core, two Cortex-A710, another two Cortex-A715, and finally one Cortex-X3. Of these *big* cores, the X3 stands out as it is the most powerful one of the set reaching up to 3.36 GHz compared to the A7XX cores that run at up to 2.8 GHz.

TABLE I: Kryo CPU configuration

ID	Type	Frequency (GHz)
0	A510	2.016
1	A510	2.016
2	A510	2.016
3	A710	2.803
4	A710	2.803
5	A715	2.803
6	A715	2.803
7	X3	3.360

In addition to the CPU, the SoC incorporates a dedicated Qualcomm Adreno 740 GPU, supporting single and half floating-point precision execution (GPU16 and GPU32 execution modes), and a dedicated NPU branded by Qualcomm as the Hexagon Processor, capable of executing both integer and half-precision float computations. Publicly available specifications for the GPU architecture are scarce; the only detailed internal information comes from a third-party blogger's analysis<sup>1</sup>. From this analysis, it is deduced that the GPU comprises 12 Shader Processor units running at up to 719 MHz, a configuration also corroborated by internal Android system configuration files.

The SoC also includes a dedicated NPU featuring specialized units for tensor, scalar, and vector operations, all

connected to a shared internal memory. This shared memory is crucial for reducing data transfer latency between these execution units, as the primary feature of the Hexagon is its ability to utilize Micro Tile Inferencing. This technique involves partitioning the AI model layers and dispatching each specific operation (tensor, scalar, or vector) to the corresponding dedicated execution unit for parallel and optimized execution.

# B. Software environment

To fully exploit the available heterogeneous hardware resources, developers utilize the LiteRT framework to integrate AI functionalities into their applications. Since LiteRT natively executes .tflite models, a mandatory conversion step is required for models originally developed in frameworks like PyTorch. This conversion is performed externally on a host machine before deployment to the target device. The final tflite model is obtained via a multi-step pipeline: first, using PyTorch's export utilities to generate the intermediate .onnx format, and subsequently employing Katsuya Hyodo's onnx2tf package for conversion to .tflite. Although LiteRT offers a direct conversion path via its ai edge torch package, this feature is still in early development and lacks broad model support; therefore, the ONNX-intermediate pipeline was selected. Crucially, the onnx2tf toolchain allows for the explicit selection of different model quantization schemes, as summarized in Table II.

TABLE II: Quantization reference

	Dototypo				
Name	Datatype				
rvanie	I/O	Operation	Activation	Weight	
float32	FP32	FP32	FP32	FP32	
float16	FP32	FP32	FP32	FP16	
int_quant	FP32	INT8	INT8	INT8	
int_quant_int16_act	FP32	INT8	INT16	INT16	
full_int_quant	INT8	INT8	INT8	INT8	
full_int_quant_int16_act	INT16	INT8	INT16	INT16	
dynamic_range_quant	FP32	Mixed	FP32	Mixed	

The quantization employed in this study is post-training quantization. Specifically, static quantization was used, where model weights are converted to the target data type (e.g., INT8) offline, resulting in a model where weights are fixed and directly used in layer operations. In contrast, Dynamic Quantization (represented later as *DYN*) uses "dynamic-range operators" <sup>2</sup> that only quantize the activations to 8-bit integer precision at runtime, immediately before the computation takes place. The weights themselves are typically stored in 8-bit precision but are often cast back to float precision briefly during computation. This scheme incurs a runtime overhead but is faster than FP32 and often offers better accuracy preservation than fully static methods.

Even though many integer widths can be used for operations, weights and activations when saving the model and are

<sup>&</sup>lt;sup>1</sup>Adreno 740 info from Kurnal's blog:https://kurnal.xlog.app/SM8550

<sup>&</sup>lt;sup>2</sup>Dynamic operators in LiteRT: https://ai.google.dev/edge/litert/models/post\_training\_quantization#dynamic\_range\_quantization

actually supported by the *Tensor* class in LiteRT, there are no optimized implementations of operations for 16 bit integers<sup>3</sup>.

In order to facilitate the experimentation a small Android application has been developed that runs the models and stores inference results and speeds. Starting from LiteRT version 2.0 is planned to change to LiteRT Next, which will make previous applications incompatible due to changes in the API. As of version 2.0.2 of LiteRT, the pipeline to run models in the NPU does not work properly<sup>4</sup>, so for this paper version 1.4 was also needed to be able to use this accelerator.

To successfully evaluate performance across the entire heterogeneous architecture, a mixed framework approach was needed due to software compatibility constraints. Specifically, CPU and GPU workloads were executed using the LiteRT Next API, which offered superior control over these units, while NPU workloads required the use of the more stable standard LiteRT framework. This methodological split allows for the comprehensive benchmarking of each accelerator's capabilities, as detailed in Table III.

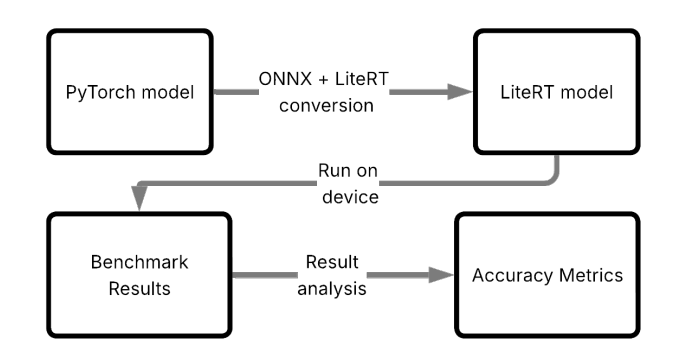
TABLE III: LiteRT version requirements

Device	LiteRT version
CPU	2.0.2
GPU	2.0.2
NPU	1.4.0

#### III. METHODOLOGY

The experimental workflow follows a multi-stage model preparation pipeline, as illustrated in Figure 1. First, models of all available sizes were sourced from official repositories: the PyTorch torchvision<sup>5</sup> module for the ResNet family, and the Ultralytics<sup>6</sup> website for the YOLO family. The core preparation pipeline consists of two conversion steps: (1) The PyTorch models are first converted into the intermediate ONNX format using PyTorch's built-in export utilities; (2) the ONNX models are then converted to the final TFLite (.tflite) format using the onnx2tf tool. This last conversion is also where the quantization of the model is performed, by default the convert function of onnx2tf outputs the model in floating point precision with 32 and 16 bit widths. In order to obtain the other variants shown in table II additional parameters must be passed to the *convert* function specifying that dynamic and integer quantizations are wanted as well<sup>7</sup>.

Fig. 1: Experimental Workflow and Model Preparation Pipeline



Finally, the last phase involved the quantitative assessment of the obtained classification and detection results to determine model accuracy. For the YOLO models, the most common accuracy metric is mean average precision (mAP) directly obtained from the Python package *pycocotools*. For ResNet, the top-1 percentage metric is also calculated by computing how many of the total predictions recorded match the ground truth for the image class.

# IV. RESULTS

Before presenting the results obtained for the ResNet image classification and YOLO object detection models, some observations are necessary. Firstly, the Table IV summarizes the acronyms used throughout the following subsections to refer to variants of precision, device and quantization used in the experimentation. Secondly, the fp32-bit model executed on the CPU on a single thread is considered as a baseline which will serve as reference for speed-up and accuracy loss comparisons. And finally, the accuracy metric depends on the model evaluated: Top 1 accuracy for ResNet, and the mean Average Precision (mAP) for YOLO.

TABLE IV: Acronym correspondence

	Acronym	Meaning
	CPU-SC	Single threaded execution
	CPU-MC	Multithreaded execution
Davisa	GPU32	GPU execution with FP32 bit precision
Device	GPU16	GPU execution with FP16 bit precision
	NPU	NPU Execution
	FP32	Floating Point 32 bits
	FP16	Floating Point 16 bits
	INT8	Integer 8 bits
Quantization	FINT8	Full Integer 8 bits
	INT16	Integer 16 bits
	FINT16	Full Integer 16 bits
	DYN	Dynamic

# A. ResNet

Table V presents the inference time measured in milliseconds (ms) for the different quantization and device variants. As the data shows, the 16-bit integer variant exhibits very poor

<sup>&</sup>lt;sup>3</sup>LiteRT documentation states lack of optimized INT16 kernels: https://ai.google.dev/edge/litert/models/post\_training\_integer\_quant\_16x8# evaluate\_the\_models

<sup>&</sup>lt;sup>4</sup>LiteRT Commit 34682d3 https://github.com/google-ai-edge/LiteRT/issues/3360#issuecomment-3335190874

<sup>&</sup>lt;sup>5</sup>ResNet models in *torchvision*: https://docs.pytorch.org/vision/main/models/resnet.html

<sup>&</sup>lt;sup>6</sup>Ultralytics' website: https://docs.ultralytics.com/es/models/ #featured-models

<sup>&</sup>lt;sup>7</sup>onnx2tf parameter documentation: https://github.com/PINTO0309/onnx2tf?tab=readme-ov-file#in-script-usage

performance (high latency), a trend observed even across different model sizes. Therefore, these quantizations are excluded from the analysis for the remainder of this section. Results also show the clear dominance of the NPU as the fastest executing device, followed by the GPU and lastly the CPU.

TABLE V: ResNet18 Average inference time (ms)

	CPU-SC	CPU-MC	GPU32	GPU16	NPU
FP32	79.06	26.34	13.68	5.54	1.20
FP16	79.31	26.52	15.71	5.61	1.19
INT8	23.26	5.63	21.77	22.68	0.61
INT16	791.35	798.39	831.95	857.21	882.30
FINT8	23.06	60.36	32.57	32.48	0.51
FINT16	883.34	883.18	883.50	883.16	880.98
DYN	32.31	7.43	40.42	37.14	37.14

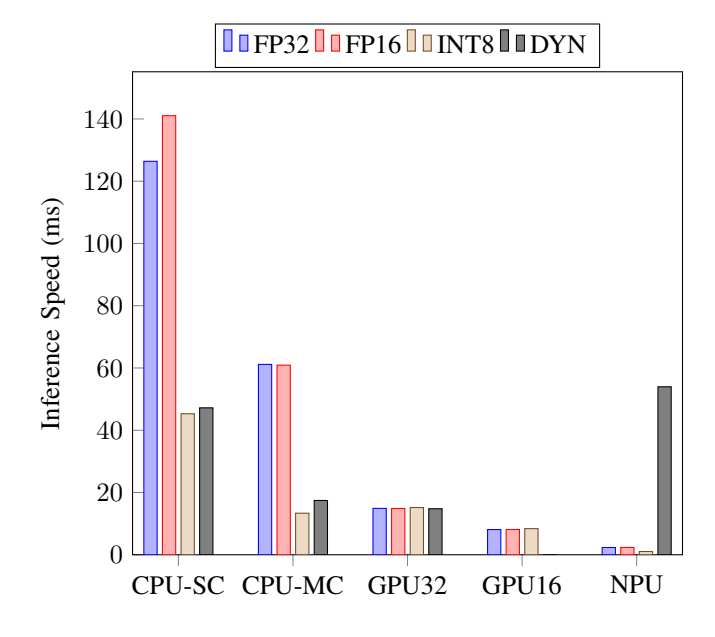
Table VI shows the Top-1 classification accuracy observed during ResNet18 model inference, varying the quantization scheme and the target device. Almost all variants achieve satisfactory accuracy, close to 69%. The single notable exception is the FINT8 variant, which reaches a drastically low Top-1 accuracy of only 0.08%. Therefore, this variant is also excluded from the remaining experimentation.

TABLE VI: ResNet18 Top1 accuracy

	CPU-SC	CPU-MC	GPU32	GPU16	NPU
FP32	68.81	68.81	68.81	68.8	68.82
FP16	68.82	68.82	68.82	68.79	68.81
INT8	65.87	65.87	65.87	65.87	65.96
INT16	65.95	65.95	65.95	65.95	65.95
FINT8	0.08	0.08	0.09	0.09	0.08
FINT16	65.95	65.95	65.95	65.95	65.95
DYN	68.71	68.71	68.71	68.71	68.71

Consistent with the previous results, Figure 2 shows the inference times for the ResNet50 model. Once again, the NPU demonstrates superior speed across the board (INT8 quantization), achieving over 120× faster inference than the CPU-SC. The exception to this performance trend is Dynamic Quantization (DYN), which is significantly slower on the NPU than the regular quantizations. This anomaly is explained by the nature of the dynamically quantized model: it is not uniformly quantized but contains layers of different precisions. While the CPU efficiently handles these mixed precisions, the NPU accelerator lacks native support for such dynamic data type conversion. Consequently, the model must rely on the CPU to perform casting operations, requiring costly data transfers between the NPU and CPU for each precision change. This overhead drastically increases the overall latency, negating the potential speed-up of the lower-precision operations on the accelerator. This outcome reinforces the conclusion that the NPU is optimized for acceleration using data pre-calculated ahead of time, not for operations computed at runtime.

Fig. 2: ResNet50 inference speeds across devices & quantizations



Focusing on CPU performance (see Table VII), the analysis revealed that the multithreaded speed-up (CPU-MC, utilizing the 8 available cores) was significantly lower than expected. The highest acceleration was achieved with INT8 quantization, reaching a factor of  $3.4\times$ , which suggests that the asymmetric multicore architecture significantly limits scalability.

TABLE VII: Multithreaded vs single threaded execution (ms) and speed-up in ResNet50

	CPU-SC	CPU-MC	Speed-up
FP32	126.4	61.2	2.1x
FP16	141.1	60.9	2.3x
INT8	45.3	13.4	3.4x
DYN	47.2	17.4	2.7x

On the GPU side, we observe that quantization hardly affects inference times (see Table VIII). Instead, the largest performance impact stems from the GPU's operating mode (FP32 vs. FP16), resulting in speed-ups approaching  $2\times$  if the GPU is configure to operate as GPU16.

TABLE VIII: GPU FP32 vs FP16 execution (ms) in ResNet50

	GPU32	GPU16
FP32	14.9	8.1
FP16	14.86	8.12
INT8	15.17	8.39
DYN	14.78	8.13

The table IX presents accuracy variation when quantizing the model. Using half precision floating point instead of single precision has practically no impact on the accuracy figures. Meanwhile, quantizing the model from fully fp32 to integer or dynamic has a greater impact.

TABLE IX: ResNet50 Top1 accuracy (%)

	CPU-SC	CPU-MC	GPU32	GPU16	NPU
FP32	79.09	79.09	79.06	79.09	79.1
FP16	79.1	79.1	79.1	79.06	79.1
INT8	78.68	78.73	78.68	78.68	78.77
DYN	78.9	78.91	78.9	-	78.94

The analysis of quantization impact reveals a clear correlation between model size and accuracy preservation. As shown in Table X, the accuracy loss incurred by INT8 quantization decreases significantly as the model complexity increases (from 2.94% for ResNet18 down to  $\leq 0.5\%$  for larger variants). This trend confirms that larger models mitigate the information loss associated with reduced data width due to their deeper feature extraction capabilities. In contrast, Dynamic Quantization (DYN) consistently introduces negligible loss.

TABLE X: Summary of Top-1 Accuracy Loss by Quantization vs. FP32 (%)

Quant.	ResNet18	ResNet34	ResNet50	ResNet101	ResNet152
INT8	2.94%	0.50%	0.41%	0.01%	0.20%
DYN	0.10%	0.04%	0.19%	0.00%	0.07%

Furthermore, Table XI demonstrates that converting the original single-precision floating-point model (PyTorch) to the LiteRT framework inherently leads to a conversion-related accuracy loss, regardless of the subsequent quantization applied. This loss ranges between 0.83% and 1.77%, suggesting that discrepancies in the inner workings and operation implementations across the frameworks prevent a perfect 1:1 conversion. This factor must be considered when evaluating the overall accuracy degradation.

TABLE XI: Precision lost (Top-1) due to framework conversion(LiteRT vs. PyTorch) (%)

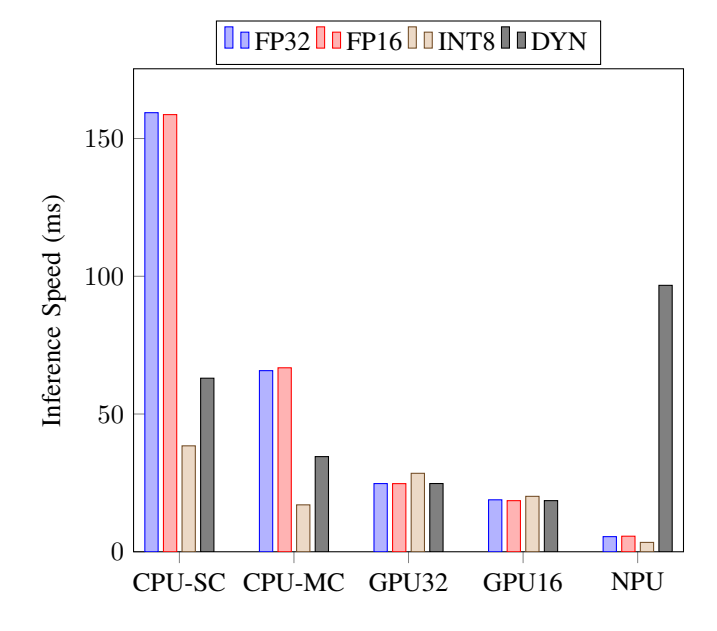
Model	ResNet18	ResNet34	ResNet50	ResNet101	ResNet152
Lost	0.95%	0.83%	1.77%	1.16%	0.98%

# B. YOLOv8

The results for YOLOv8 show the same pattern as ResNet: using the accelerators makes the processing much faster. However, YOLOv8 takes longer (has higher latency) than ResNet. This is because YOLOv8 is a more complex network designed for a harder task (object detection) compared to ResNet's simpler one of just image classification.

Figure 3 shows the inference time involve in YOLO8n model varying devices and quantization. The NPU offers the best performance in comparison with devices such as CPU or GPU.

Fig. 3: YOLOv8n inference speeds across devices & quantizations



Shifting the focus to accuracy, as can be seen in Table XII, the integer quantized variants suffer more degradation than in ResNet model. Lower precision, like INT8 quantization, significantly hurts object detection models (YOLOv8) because this task demands more information (localization and classification) than simpler tasks like image classification. The dynamic quantization (DYN) method performs much better, losing a maximum of only 0.1 mAP across the models, which is negligible. Conversely, INT8 quantization causes a large performance drop, averaging about 6.5 mAP points lost across all model sizes.

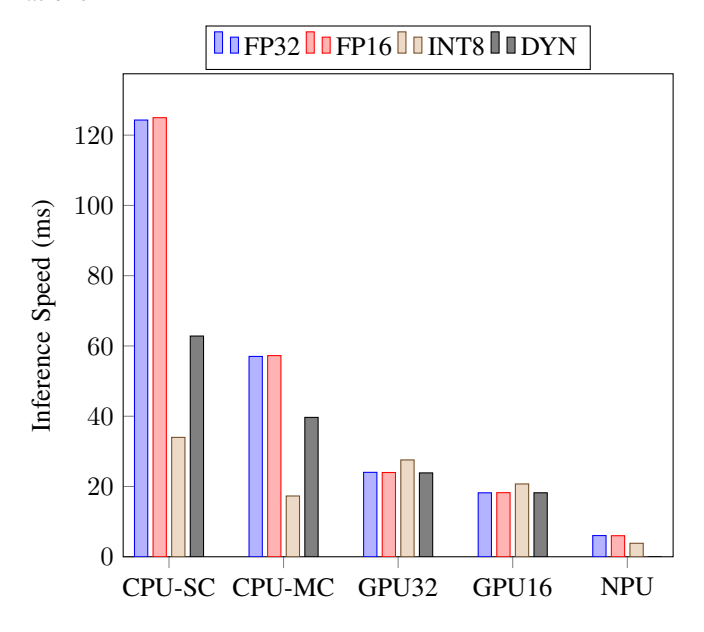
TABLE XII: YOLOv8 accuracy loss (mAP) compared to FLOAT32 precision

Quant.	YOLOv8n	YOLOv8s	YOLOv8m	YOLOv8l	YOLOv8x
INT8	6.5	6.2	6.2	7.5	6.1
DYN	0.1	0.0	0.0	0.1	0.1

# C. YOLO11

With YOLO11 being an upgraded version of YOLOv8 it is expected to behave similarly but come with some improvements compared to its predecessor. The Figure 4 presents the newer YOLO11 inference times. It generally behaves like YOLOv8 but shows minor changes: CPU inference is slightly faster, while GPU speeds are nearly identical. Execution on the NPU is marginally slower for both float and INT8 models, and dynamic quantization fails to run entirely on the NPU. This performance shift is likely due to YOLO11's more complex architecture and new layers compared to its predecessor.

Fig. 4: YOLO11n inference speeds across devices & quantizations



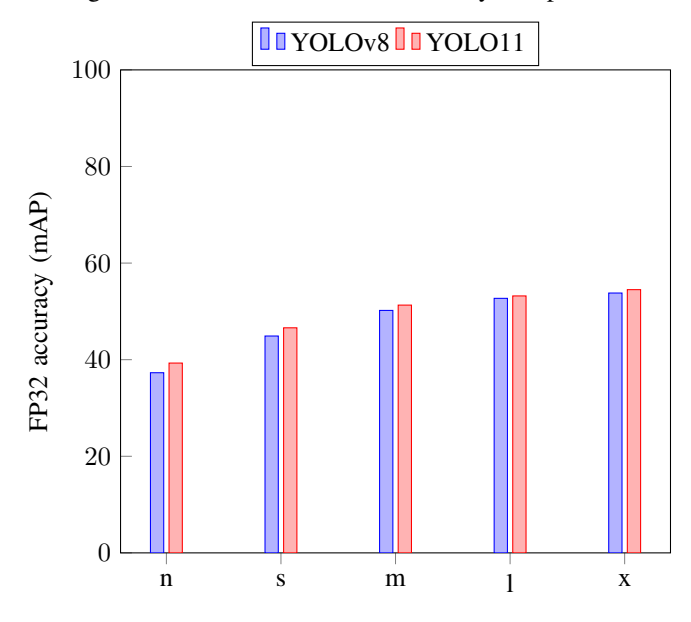
Accuracy results for YOLO11 match the general trend seen in YOLOv8 as shown in Table XIII. However, integer quantization (INT8) in YOLO11 models causes a slightly greater loss in accuracy, averaging around 7.2 mAP points across the models. As with the previous version, dynamic quantization (DYN) maintains an almost perfect accuracy result, with a maximum loss of just 0.2 mAP.

TABLE XIII: YOLO11 accuracy loss (mAP) compared to FLOAT32 precision

Quant.	YOLO11n	YOLO11s	YOLO11m	YOLO111	YOLO11x
INT8	6.6	6.8	6.7	8.7	7.2
DYN	0.1	0.1	0.1	0.2	0.1

Finally, it isimportant to note that YOLO11 exhibits a minor degradation in accuracy compared directly against its original PyTorch version, caused by the conversion to the required format for the LiteRT framework. This nominal loss, typically ranging between 0.2 and 0.4 mAP percentage points, implies that the novel layers incorporated into the YOLO11 architecture present a greater challenge for effective conversion into the LiteRT runtime environment. Despite this minor conversion-induced discrepancy, the empirical evidence confirms that YOLO11 provides a superior overall performance in FP32 accuracy across all model scales when benchmarked against YOLOv8 (as validated by the data presented in Figure 5). Thus, YOLO11 establishes itself as the more precise model for object detection tasks.

Fig. 5: YOLO11 vs YOLOv8 accuracy comparison



#### D. Discussion

After analyzing the results obtained from all the executions of the different models in the various devices, the most suitable accelerator is the NPU, which achieves impressive speed-ups in the smaller models approximately  $47\times$  in YOLOv8n and  $130\times$  in ResNet18, and this ratio generally increases with the model size, reaching up to  $298\times$  speed-up in YOLOv8x versions. Table XIV summarizes the speed-up achieved for each model and quantization variant.

TABLE XIV: NPU execution speed-ups

		FP32	FP16	INT8	DYN
	18	65.9x	66.4x	129.6x	2.1x
	34	89.2x	88.2x	190x	3.7x
Resnet	50	54.3x	53.3x	121.5x	2.3x
	101	64.9x	63.6x	149.7x	3x
	152	70x	67.5x	164.1x	-
	n	29x	28.2x	46.8x	1.6x
YOLOv8	s	60.2x	60.5x	128.3x	2.9x
	m	77.6x	81.6x	209.4x	-
	1	99.5x	100.7x	277.6x	-
	x	98.2x	100x	298x	-
YOLO11	n	20.6x	20.8x	32.4x	-
	s	44.2x	41.5x	76.5x	-
	m	62.3x	64.9x	146.1x	-
	1	71.2x	72.5x	160.3x	-
	x	72.9x	72.6x	173.9x	-

Another important observation is that the dynamically quantized model seems to have some troubles across all models, due to reduced speed-ups in comparison with other quantization options or even failure to run. Scalability is also observed when model size increases as acceleration grows, being more impressive for YOLO8 family.

Focusing on CPU performance, Table XV clearly demonstrates that the maximum achievable speed-up with multithreading is predominantly driven by integer precision (INT8), consistently ranging between  $10\times$  and  $15\times$  faster execution,

while floating-point precisions achieves a modest  $2\times$  to  $3\times$  acceleration. The multi-threading efficiency varies by model family and size: ResNet models exhibit a decreased speedup in INT8 as model size increases, whereas YOLO models demonstrate the opposite trend, achieving a better speed-up as they scale up.

TABLE XV: Multithreaded execution speed-ups

		FP32	FP16	INT8	DYN
	18	3x	3x	14x	10.6x
	34	3.1x	3.1x	15.1x	12x
Resnet	50	2x	2x	9.5x	7.2x
	101	2.2x	2.1x	9.2x	7.2x
	152	2.2x	2.3x	9.4x	7.6x
	n	2.4x	2.4x	9.4x	4.6x
	S	2.3x	2.3x	11.1x	6.7x
YOLOv8	m	2.4x	2.4x	12.5x	7.5x
	1	2.3x	2.7x	12.8x	9.7x
	X	2.7x	2.1x	13.4x	10.1x
	n	2.2x	2.2x	7.2x	3.1x
	S	2.1x	2.1x	10.4x	4.3x
YOLO11	m	2.4x	2.3x	13.1x	6.2x
	1	2.6x	2.3x	13.4x	6.6x
	X	2.2x	2.1x	12.5x	7.3x

Finally, the analysis on GPU device presented in the Table XVI reveals that the best performance rates are found in GPU16 mode. In contrast to the CPU, variations in precision (FP32, FP16, INT8, DYN) have a marginal impact on the speed-up factor, suggesting that performance is constrained other factors such as memory bandwidth or arithmetic complexity. Nevertheless, results suggests that FP16 is frequently the optimal choice, effectively balancing speed and precision on the GPU. Regarding scaling, the YOLO models demonstrate superior efficiency on the GPU, with the largest models (reaching up-to 39× for YOLOv8x) achieving the highest acceleration, while ResNet models maintain a more consistent speed-up across their sizes. Speedup results indicates that larger models take more advantage of being executed at half precision than smaller models, this is in accordance with how GPUs behave in regular tasks, as to take full advantage of this device the workload needs to be massively parallel like with these larger models.

TABLE XVI: GPU16 execution speed-ups

		FP32	FP16	INT8	DYN
	18	17.5x	-	16.9x	-
	34	20x	20x	-	20x
Resnet	50	15.6x	15.6x	15.1x	15.6x
	101	15.8x	15.8x	15.5x	15.8x
	152	16.5x	16.5x	16.3x	16.3x
YOLOv8	n	8.5x	8.6x	8x	8.5x
	S	17.2x	17.1x	15.5x	17.1x
	m	14.6x	14.6x	13.1x	14.6x
	1	35x	34.8x	31.9x	34.9x
	X	38.3x	38.2x	34.8x	38.6x
YOLO11	n	6.8x	6.8x	6x	6.8x
	s	14x	14x	12.3x	14x
	m	23.2x	23.2x	19.3x	23.1x
	1	25.5x	25.2x	22x	25.2x
	X	30.1x	30.1x	26.5x	30.2x

Finally, selecting the optimal configuration is inherently a

challenge due to the conflicting objectives typically sought, such as achieving high accuracy alongside moderate inference times without ignoring limited power consumption constraints. To address this multi-criteria decision problem, a multi-objective optimization approach using a Pareto Front analysis is proposed. In order to avoid cluttering, only FP16 and INT8 quantizations were selected to be shown in the graphs as they are involved in the most promising configurations.

Fig. 6: Pareto Front ResNet

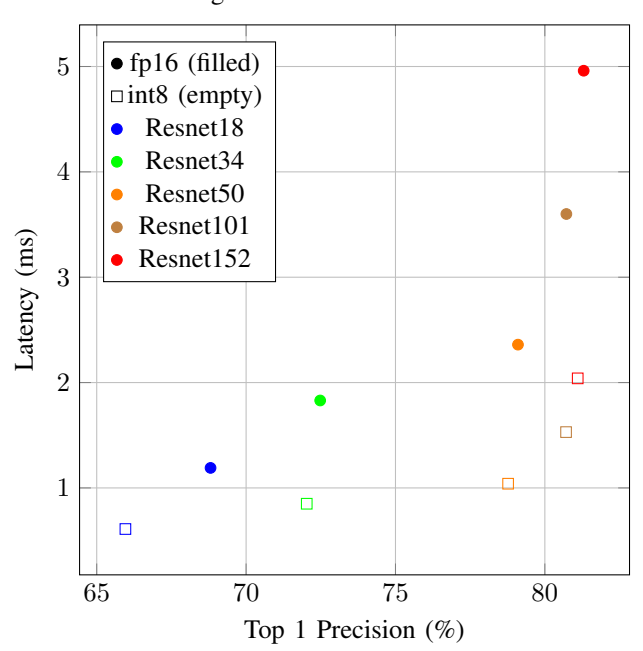
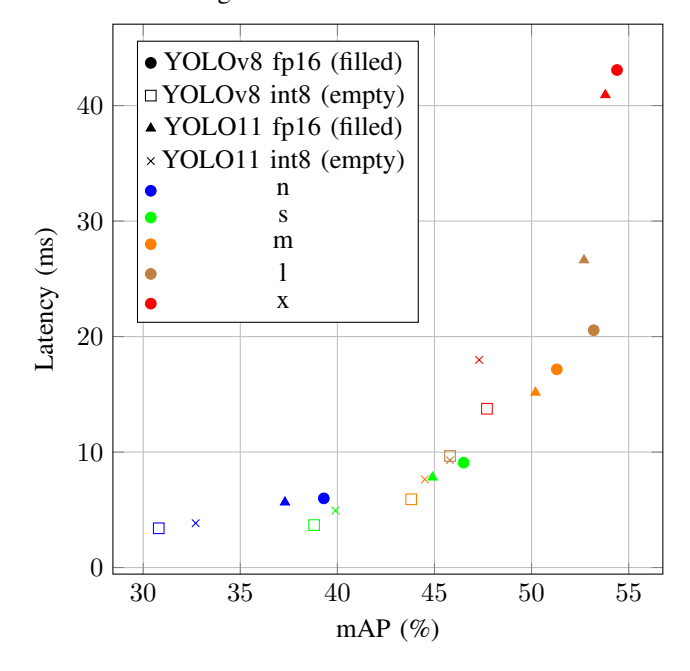


Fig. 7: Pareto Front YOLO



Figures 6 and 7 present the resulting Pareto Front, which displays the non-dominated trade-offs between accuracy and

inference time across the two selected quantization schemes and deployment devices. This analysis emphasizes the best possible compromises available to system designers by clearly distinguishing between superior and sub-optimal configurations. It can be deduced that in the case of ResNet (see Figure 6) INT8 is clearly the way to go, as the latency decrease compensates the accuracy loss of using integer precision. In contrast, for YOLO (Figure 7), though, as these models suffer much more from integer related accuracy loss, these variants of the model are further away from the optimum front. Another key takeaway is that YOLO11 seems to outperform YOLOv8 in the smaller sizes where the accuracy increase makes it fare better at the cost of slightly increased latency, this advantage goes away the bigger the model is and consequently the slower it becomes.

# V. CONCLUSIONS

This paper evaluated the performance of ResNet and YOLO models for image classification and object detection, respectively, across three devices (CPU, GPU, NPU) and four precisions in an Android tablet. The key findings are:

- The NPU is the best execution device, achieving speedups up to 120× compared to the CPU single-core baseline, confirming its essential role in low-latency edge AI.
- Optimal Quantization is a trade-off, and the choice between FP16 and INT8 depends on the model:
  - INT8 is the optimal precision in ResNet, as its speed gain on the NPU over the CPU outweighs its minimal accuracy loss.
  - Quantization provides negligible speed benefits over FP16 execution in GPU, making it the preferred choice for balancing speed and full accuracy on the GPU.
- Regarding model Performance & Scaling:
  - YOLO11s represents a strong candidate on the Pareto Front, offering a superior speed/accuracy compromise for object detection with FP16 quantization.
  - YOLO11 provides an overall accuracy gain over YOLOv8 for smaller model sizes, despite its slightly increased complexity.

From the system limitations perspective, we have identified that Dynamic Quantization (DYN) fails on the NPU due to lack of native support, and CPU multi-threading scalability is poor ( $\approx 3.4 \times$  max speed-up) due to the asymmetric core architecture. As future work, we plan to complete a Pareto Analysis that integrates power consumption to finalize the multi-objective optimization (accuracy, latency, power efficiency) and to mitigate NPU issues such as DYN compatibility to eliminate the  $\approx 1\%$  framework conversion accuracy loss observed with LiteRT. Furthermore, we intend to generalize these findings by studying the behaviour of additional models included in the MLPerf benchmark suite, specifically those

designed for tasks such as natural language processing or image segmentation.

#### **FUNDING**

This paper has been partially funded by the EU (FEDER), the Spanish MINECO under grants PID2021-126576NB-I00 and PID2024-158311NB-I00 funded by MCIN/AEI/10.13039/501100011033 and by European Union "ERDF A way of making Europe" and the NextGenerationEU/PRT.

# REFERENCES

- Z. Yang, K. Adamek, and W. Armour, "Double-exponential increases in inference energy: The cost of the race for accuracy," 2024. [Online]. Available: https://arxiv.org/abs/2412.09731
- [2] C.-J. Wu, R. Raghavendra, U. Gupta, B. Acun, N. Ardalani, K. Maeng, G. Chang, F. A. Behram, J. Huang, C. Bai, M. Gschwind, A. Gupta, M. Ott, A. Melnikov, S. Candido, D. Brooks, G. Chauhan, B. Lee, H.-H. S. Lee, B. Akyildiz, M. Balandat, J. Spisak, R. Jain, M. Rabbat, and K. Hazelwood, "Sustainable ai: Environmental implications, challenges and opportunities," arXiv preprint arXiv:2111.00364, 2022. [Online]. Available: https://arxiv.org/abs/2111.00364
- [3] Google LLC, "Google environmental report 2023," Google LLC, Environmental Report, 2023. [Online]. Available: https://www.gstatic. com/gumdrop/sustainability/google-2023-environmental-report.pdf
- [4] Meta Platforms, Inc., "Meta sustainability report 2023," Meta Platforms, Inc., Sustainability Report, 2023. [Online]. Available: https://sustainability.atmeta.com/resources/
- [5] S. Moreschini, E. Younesian, D. Hästbacka, M. Albano, J. Hošek, and D. Taibi, "Edge to cloud tools: A multivocal literature review," *Journal of Systems and Software*, vol. 210, p. 111942, 2024. [Online]. Available: https://www.sciencedirect.com/science/article/pii/S0164121223003370
- [6] S. S. Gill, H. Wu, P. Patros, C. Ottaviani, P. Arora, V. C. Pujol, D. Haunschild, A. K. Parlikad, O. Cetinkaya, H. Lutfiyya et al., "Modern computing: Vision and challenges," *Telematics and Informatics Reports*, vol. 13, p. 100116, 2024.
- [7] A. Ahmed Murtaza, A. Saher, M. Hamza Zafar, S. Kumayl Raza Moosavi, M. Faisal Aftab, and F. Sanfilippo, "Paradigm shift for predictive maintenance and condition monitoring from industry 4.0 to industry 5.0: A systematic review, challenges and case study," *Results in Engineering*, vol. 24, p. 102935, 2024. [Online]. Available: https://www.sciencedirect.com/science/article/pii/S2590123024011903
- [8] W. Fei, H. Ohno, and S. Sampalli, "A systematic review of iot security: Research potential, challenges, and future directions," ACM computing surveys, vol. 56, no. 5, pp. 1–40, 2023.
- [9] OpenAI, "Introducing ChatGPT," 2022. [Online]. Available: https://openai.com/index/chatgpt/
- [10] V. J. Reddi, C. Cheng, D. Kanter, P. Mattson, G. Schmuelling, C.-J. Wu, B. Anderson, M. Breughe, M. Charlebois, W. Chou, R. Chukka, C. Coleman, S. Davis, P. Deng, G. Diamos, J. Duke, D. Fick, J. S. Gardner, I. Hubara, S. Idgunji, T. B. Jablin, J. Jiao, T. S. John, P. Kanwar, D. Lee, J. Liao, A. Lokhmotov, F. Massa, P. Meng, P. Micikevicius, C. Osborne, G. Pekhimenko, A. T. R. Rajan, D. Sequeira, A. Sirasao, F. Sun, H. Tang, M. Thomson, F. Wei, E. Wu, L. Xu, K. Yamada, B. Yu, G. Yuan, A. Zhong, P. Zhang, and Y. Zhou, "Mlperf inference benchmark," in *Proceedings of the ACM/IEEE 47th Annual International Symposium on Computer Architecture*, ser. ISCA '20. IEEE Press, 2020, p. 446–459. [Online]. Available: https://doi.org/10.1109/ISCA45697.2020.00045
- [11] K. He, X. Zhang, S. Ren, and J. Sun, "Deep Residual Learning for Image Recognition," in *Proceedings of the IEEE Conference on Computer Vision and Pattern Recognition (CVPR)*, 2016, pp. 770–778, ganador del ILSVRC 2015 en clasificación, detección y segmentación. [Online]. Available: https://arxiv.org/abs/1512.03385
- [12] L. T. Ramos and A. D. Sappa, "A decade of you only look once (yolo) for object detection: A review," 2025. [Online]. Available: https://arxiv.org/abs/2504.18586